NUMERICAL SIMULATION OF PENETRATION PROBLEMS IN GEOTECHNICAL ENGINEERING WITH THE PARTICLE FINITE ELEMENT METHOD (PFEM)

LLUÍS MONFORTE[1], JOSEP MARIA CARBONELL[1,2], MARCOS ARROYO[1] AND ANTONIO GENS[1]

[1] Universitat Politècnica de Catalunya - BarcelonaTech
Campus Norte UPC, 08034 Barcelona, Spain
e-mail: antonio.gens@upc.edu

[2] Centre Internacional de Mètodes Numèrics en Enginyeria (CIMNE)
Universitat Politècnica de Catalunya
Campus Norte UPC, 08034 Barcelona, Spain

Key words: PFEM, Porous media, soil mechanics, penetration tests.

Abstract. This paper highlights a computational framework for the numerical analysis of saturated soil-structure interaction problems. The variational equations of linear momentum and mass balance are obtained for the large deformation case. These equations are solved using the Particle Finite Element Method. The paper concludes with a benchmark test and the analysis of a penetration test.

1 INTRODUCTION

Penetration tests -such as cone penetration test (CPT), T-Bar, and others- are widely used in geotechnical engineering to determine soil properties. Using a realistic description of the soil behavior (e.g. elasto-plastic effective stress response) increases both the range of conditions for and the precision of test interpretation. The downside is that a number of material non-linearities are added to a problem that already features a severe geometric non-linearity.

Finite element method is well suited to include all sort of non-linearities. However, when a Lagrangian formulation is employed -typically when a path dependent material model is used- the mesh may experience severe distortion, leading to numerical inaccuracies and even rendering the calculation impossible. In order to alleviate this problem several numerical techniques based on FEM have been proposed (adaptive methods, Arbitrary Lagrangian-Eulerian,...).

In this work, the Particle Finite Element Method (PFEM) is employed to simulate the penetration of a rigid probe into the soil. The method is characterized by a particle

1

discretization of the domain: every time-step a finite element mesh -whose nodes are the particles- is build using a Delaunay's tessellation and the solution is evaluated using well shaped, low order finite elements [1, 2].

The soil-water mixture is modeled as a two-phase continuum employing a finite deformation formulation. The linear momentum and mass balance equations are written following the movement of the solid skeleton, where the unknown fields are the solid skeleton displacements and the fluid pressure ($u - p_w$ formulation). The water flow is assumed to obey a generalization of the Darcy's Law whereas a multiplicative hyperelastic-plastic constitutive response is assumed for the solid skeleton. The proposed model differs slightly from previous approaches [3, 4] in the definition of the reference configuration, in the Darcy's law and the working unknowns.

The proposed approach is assessed against a numerical benchmark example, an oedometer test, showing a good agreement with the analytical solution. Finally, the effect of the penetration rate of the CPT on the cone resistance and the excess pore pressure in a Modified Cam Clay soil is evaluated.

2 GOVERNING EQUATIONS

In this section, the governing equations of the porous media are highlighted. First, the strong form of the mass and momentum balance equations are obtained. After briefly describing the constitutive equations, the weak form of the residual is presented.

2.1 Strong form

The mass of each phase of the porous media -solid skeleton, m_s, and water, m_w,- in an arbitrary deformed domain Ω_i^{n+1} may be expressed as:

$$m_s = \int_{\Omega_i^{n+1}} \rho_s(1 - \varphi) \, d\Omega^{n+1} \tag{1}$$

$$m_w = \int_{\Omega_i^{n+1}} \rho_w \varphi \, d\Omega^{n+1}$$

where φ is the porosity and ρ_s and ρ_w are the solid and water density respectively.

Since the mass on the control volume is conserved, the material derivative of the integral is null; therefore:

$$\frac{d(m_s)}{dt} = 0 \implies \int_{\Omega_i^{n+1}} \left(\frac{\partial(\rho_s(1 - \varphi))}{\partial t} + \frac{\partial(\rho_s(1 - \varphi)v_i)}{\partial x_i} \right) d\Omega^{n+1} = 0 \tag{2}$$

$$\frac{D(m_w)}{Dt} = 0 \implies \int_{\Omega_i^{n+1}} \left(\frac{\partial(\rho_w \varphi)}{\partial t} + \frac{\partial(\rho_w \varphi \overline{v_i})}{\partial x_i} \right) d\Omega^{n+1} = 0$$

where $\frac{d}{dt}$ and $\frac{D}{Dt}$ are the material derivatives with respect to the solid and fluid phase and v and $\overline{v}$ are the solid and fluid velocities.

After some algebraic manipulation and summing both expressions, an equation for the conservation of mass in the mixture is obtained:

$$\frac{-\varphi}{K_w}\frac{dp}{dt} - \frac{v^d}{K_w} \cdot \nabla p + \nabla \cdot v + \nabla \cdot v^d = 0 \tag{3}$$

where the Darcy's velocity, v^d, has been introduced: $v^d = \varphi(\overline{v} - v)$, p is the water pressure and K_w is the water compressiblity.

The problem definition is completed with the balance of linear momentum of the mixture. Excluding inertial effects, the strong form can be expressed as:

$$\nabla \cdot \sigma + \rho g = 0 \tag{4}$$

where σ is the total Cauchy stress tensor and $\rho = (1 - \varphi)\rho_s + \varphi\rho_w$ is the density of the mixture.

According to the principle of effective stress, the total stress tensor is equal to the sum of the pore pressure and the effective stress, σ':

$$\sigma_{ij} = \sigma'_{ij} + p\delta_{ij} \tag{5}$$

2.2   Constitutive relations

A multiplicative elasto-plastic constitutive response is assumed for the solid skeleton. The integration of stresses is performed with an explicit integration scheme with adaptive sub-stepping and a correction for the yield surface drift is applied [5].

A large deformation generalization of the Darcy's Law, excluding inertial effects, may be written as:

$$v^d = \frac{K}{\rho_w g} \cdot (\nabla p + \rho_w g) \tag{6}$$

where K is the spatial permeability tensor and g is the gravity; compressions in the water pressure are considered negative. In this work, this constitutive law is stated in a spatial setting; that is, the spatial description of the permeability tensor is assumed to be constant. On the other hand, the permeability may be considered as a material property (then, the principal directions of the tensor rotate with the deformation) [4].

2.3   Residual form

The weak form of the mass conservation expression, equation (3), is expressed in the current deformed configuration; a fully implicit time-marching scheme is used:

$$R = \int_{\Omega^{n+1}} q\Big(\frac{\partial \Delta u_i^{n+1}}{\partial x_i} - \frac{\Delta p^{n+1}}{K_w}\Big)\frac{1}{J_0^{n+1}}d\Omega^{n+1} - \int_{\Omega^{n+1}} \frac{\partial q}{\partial x_i}\frac{K_{ij}}{\rho_w g}\Big(\frac{\partial p^{n+1}}{\partial x_j} + \rho_w g_j\Big)\frac{\Delta t}{J_0^{n+1}}d\Omega^{n+1} \tag{7}$$

where q is the virtual Cauchy water pressure, $\Delta u^{n+1} = u^{n+1} - u^n$ and $\Delta p^{n+1} = p^{n+1} - p^n$.

In the other hand, the residual of the mechanical problem, equation (4), is:

$$R = \int_{\Omega^{n+1}} \frac{\partial w_i}{\partial x_j} \sigma_{ji} d\Omega^{n+1} + \int_{\Omega^{n+1}} w_i g_i \rho d\Omega^{n+1} \tag{8}$$

where w is the virtual displacement.

The tangent matrices of the problem are derived performing a pull-back of the residual to the initial configuration and all large-strains terms are considered. It is worth noting that the usual small strains equations of computational geomechanics may be obtained from the presented formulation by neglecting second order terms of the residual and tangent matrices.

In the present implementation, both equations are solved in a monolithic approach; the space is discretized with linear triangles and the same shape functions are used both for displacements and water pressure. This type of element may produce spurious oscillations in the pore pressure field when the fluid is almost incompressible and in the nearly impermeable situation as a result of failure to satisfy the inf-sup condition. In order to alleviate these oscillations, a Fluid Pressure Laplacian stabilization term is added to the mass balance equation [6].

The problem is completed with the contact constraints, that are imposed with a penalty method.

3   NUMERICAL METHOD

A typical solution algorithm with the Particle Finite Element Method involves the following steps:

1. Discretize the domain with a Finite Element mesh. Define the shape and movement of the rigid structure.

2. Identify the external boundaries. Search the nodes that are in contact with the rigid structure and initialize the contact conditions.

3. Compute some time-steps of the coupled hydro-mechanical problem using a monolithic solver.

4. Construct a new mesh. This step may include introducing new particles on the domain in areas with large plastic dissipation, generate a new Delaunay's tessellation and perform some mesh smoothing; then, state variables are interpolated from the previous mesh to the new one.

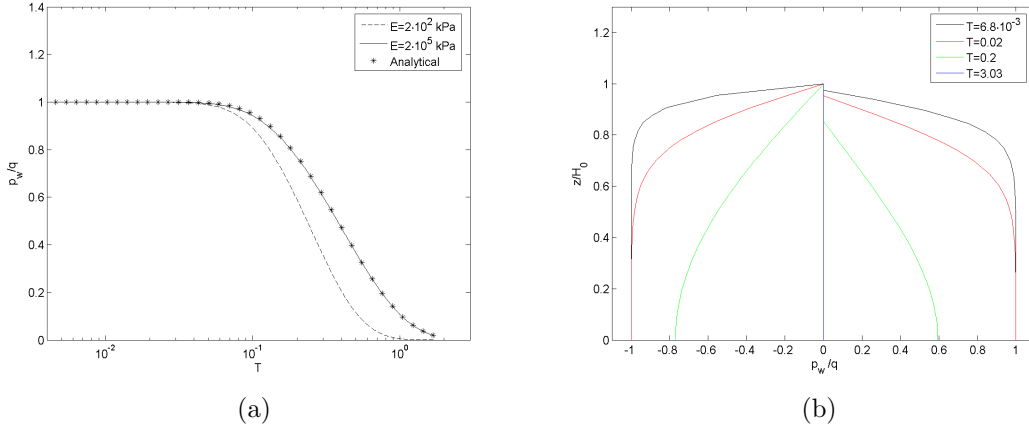5. Go back to step 2 and repeat the solution process for the next time-steps.

(a)
(b)

Figure 1: Oedoemeter test. Dissipation curves for two sets of parameters at the center of the oedometer and (b) isochrones: vertical profiles of the water pressure for $E = 2 \cdot 10^5$ kPa (left) and $E = 2 \cdot 10^2$ kPa (right).

4 NUMERICAL EXAMPLES

In this section, first a benchmark example is presented to assess the implementation; then, some results on the influence of the penetration velocity of CPT on some geotechnical quantities of interest are presented.

4.1 Oedometer test

The first example corresponds to an oedometer test in a weightless soil. This test consists on applying a vertical load to a soil sample whose lateral displacements are prevented; drainage is only allowed through the top of the sample. Small strains analytical solutions states that the key constitutive parameter that controls the pore pressure dissipation is the coefficient of consolidation, $c_v = \frac{E(1-\nu)}{(1+\nu)(1-2\nu)} \frac{K}{\rho_w g}$.

Figure 1(a) shows the variation of the water pressure at the bottom of the sample as a function of time for two sets of parameters (Young's modulus and permeability) maintaining constant the coefficient of consolidation $c_v = 2.7 \cdot 10^{-3}$ m^2/s. In the larger Young's modulus case, both displacements and deformations are small and the solution agrees well with the small strains analytical solution. The other case is different due to the severe geometric non-linearity: as consolidation takes place the height of the domain decreases; thus, the draining path length reduces, see Figure 1(b).

4.2 Penetration test

The last numerical example consists on the penetration of a smooth CPT in a Modified Cam Clay soil; the geometry and constitutive soil parameters try to mimic the example reported by Sheng et al [7].

Figure 2(a) shows the evolution of the net cone resistance in terms of penetration depth
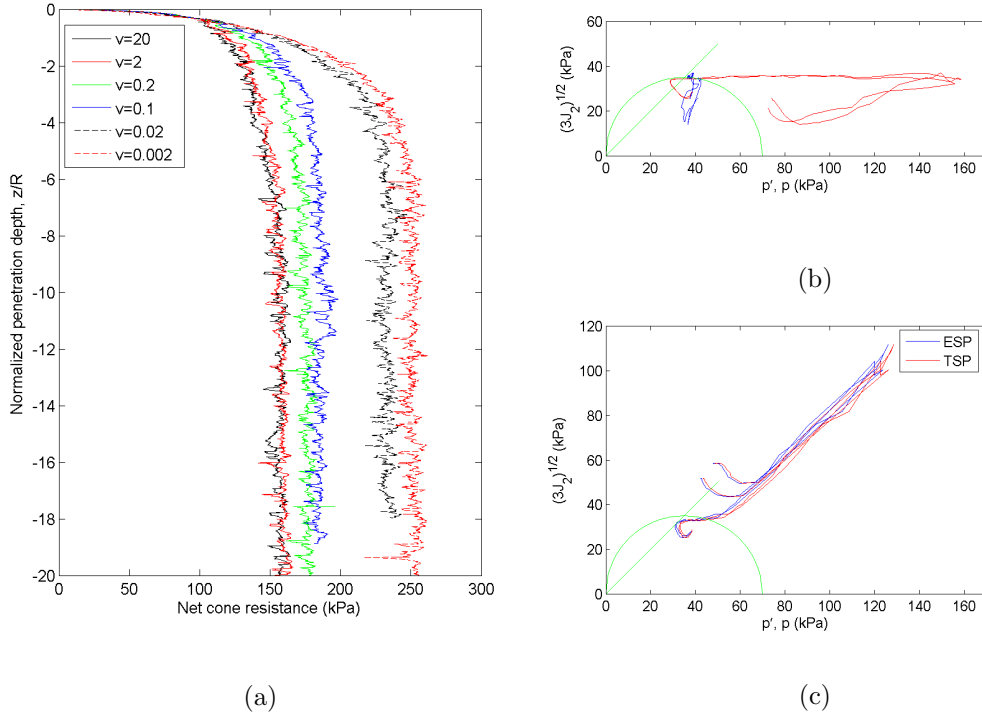
(a)

(b)

(c)

Figure 2: CPT test. Variation of the net cone resistance in terms of the penetration depth for different penetrations rates, (a). Effective stress path (ESP) and total stress path (TSP) at an horizontal distance of $\frac{R}{3}$ to the CPT shaft and a depth of 7 and 9.5 radii below the cone initial position for a penetration velocity of 20 m/s, (b), and 0.002 m/s, (c), along with the initial yield surface and the critical state line, in green. Compressions are assumed positive.

for various penetration velocities. Altough these curves present some oscillations due to the numerical method, in all cases a steady state is achieved approximately at 6 radii. These results are in good agreement with the reference solution.

The computed cone resistance varies between two limiting values; the smallest one coincides with the larger penetration rates whereas the largest one coincides with the smaller penetration rates. Figures 2(b) and 2(c) show the stress path of two typical points for a penetration velocity of 20 m/s and 0.002 m/s respectively. It can be seen that in the larger penetration velocity the effective mean stress remains approximately constant whereas large excesses of water pressure are generated; this response may be idealized as representing undrained conditions. The fact that the mean effective stress is not constant in the elastic phase is mostly due to the hyperelastic constitutive model, that couples the volumetric and deviatoric behavior, although some numerical issues (the interpolation between evolving meshes and the use of a stabilized form) may also play a role. On the other hand, for a penetration velocity of 0.002 m/s the total and effective

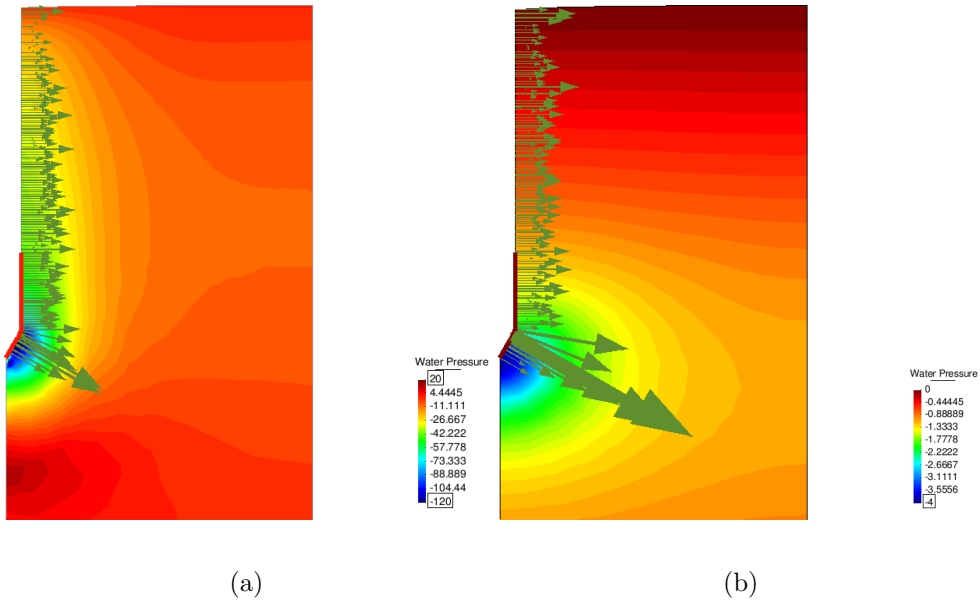(a)   (b)

Figure 3: CPT Test. Contours of the Cauchy water pressure and contact force after a penetration of 20 radii for a velocity of 20 m/s, (a), and 0.002 m/s, (b). Compression in the water pressure field are depicted with negative values.

stress path practically coincide since a limited variations on the water pressure takes place; thus, this simulation may be interpreted as the drained limit.

The water pressure profile for the larger rate, after a penetration of 20 radii, is depicted in Figure 3(a). This field exhibits its maximum value near the edge of the tip and the shaft of the CPT; from this point, it sharply decreases in the horizontal direction and below the tip; some tractions in the water pressure occur below the cone tip. Large water pressures are also encountered at the cone shaft, where shearing continues.

In the other hand, for a penetration rate of 0.002 m/s, Figure 3(b), the water pressure contour hardly varies from the initial state; the maximum (4 kPa) is observed below the cone tip.

5   CONCLUSIONS

In this work, a numerical framework for the analysis of saturated porous media undergoing large deformations has been presented. The basic balance equations and its linearized form have been described. By means of the analysis of the oedometer test it has been shown that the obtained results are accurate. Indeed using a large deformation theory may reflect results that are artificially excluded by the linear theory. Finally, a parametric analysis of the penetration velocity of a rigid probe into a Modified Cam Clay soil has been performed.

ACKNOWLEDGMENTS

REFERENCES

[1] Carbonell, J.M., Oñate, E. and Suárez, B. Modeling of ground excavation with the particle finite-element method *Journal of Engineering Mehcanics* (2010) **136**:(4) 455–463

[2] Carbonell, J.M., Oñate, E. and Suárez, B. Modelling of tunelling processes and rock cutting tool wear with the particle finite element method *Computational Mechanics* (2013) **52**(3):607–629

[3] Borja, R.I. and Alarcón, E. A mathematical framework for finite strain elastoplastic consolidation. Part I: Balance laws, variational formulation, and linearization *Comput. Methods Appl. Mech. Engrg.* (1995) **122**(1):145–171

[4] Larsson, J. and Larsson, R. Non-linear analysis of nearly saturated porous media: theoretical and numerical formulation *Comput. Methods Appl. Mech. Engrg.* (2002) **191**:3885-3907

[5] Monforte, L., Arroyo, M., Gens, A. and Carbonell, J.M. Explicit finite deformation stress integration of the elasto-plastic constitutive equations *Computer Methods and Recent Advances in Geomechanics - Proceedings of the 14th Int. Conf. of IACMAG* (2014) 267–272

[6] Preisig, M. and Prévost, J.H. Stabilization procedures in coupled poromechanics problems: A critical assessment *Int. J. Numer. Anal. Mesh. Geomech.* (2011) **35**:1207–1225

[7] Sheng, D., Kelly, R., Pineda, J. and Lachlan, B. Numerical study of rate effects in cone penetration test *3rd International Symposium on Cone Penetration Testing* (2014) 419–428